

Supporting Information

Influence of Natural Organic Matter Fouling and Osmotic Backwash on Pressure Retarded Osmosis Energy Production from Natural Salinity Gradients

NGAI YIN YIP AND MENACHEM ELIMELECH*

Department of Chemical and Environmental Engineering

Yale University

New Haven, CT 06520-8286

(*E-mail: menachem.elimelech@yale.edu)

MATERIALS AND METHODS

Membrane Characterization. The polyamide active layers transport properties (water permeability, A , and salt permeability, B) and the support layer structural parameter, S , of the hand-cast membranes were determined using a protocol adapted from our FO characterization methodology.¹ A laboratory-scaled experimental setup described in our previous studies²⁻⁴ was employed for the characterizations (Figure S1). The custom-built cell has an effective membrane area of 20.02 cm² on both sides. The feed and draw solutions were circulated in concurrent crossflow, without spacers, at a velocity of 10.7 cm/s in closed loops. An analytical balance (Denver Instruments, Bohemia, NY) recorded the draw solution weight gain, and calibrated conductivity meters measured the feed and draw solution salt concentration (Oakton Instruments, Vernon Hills, IL and Mettler Toledo, Columbus, OH, respectively). Temperature of the system was maintained at 25 ± 0.5 °C for all characterization experiments.

Characterization experiments were conducted with the membrane in PRO configuration, i.e., porous support layer facing the feed solution and active layer facing the draw solution. The experimental run consists of eight stages. In the first four stages the draw solution concentration is progressively raised while the feed solution is DI water. The water flux and reverse draw salt flux increases with each stage due to the greater salt concentration gradient and osmotic driving force across the membrane. The initial four stages are, thus, similar to the FO membrane characterization method.¹ In the fifth to eighth stages, the concentration of the draw solution is maintained constant while the feed solution concentration is increased stepwise. In PRO the porous support layer is facing the feed solution, unlike FO where the support layer faces the draw solution.^{4,5} Upon the addition of salt to the feed solution, the osmotic driving force for the transport of water across the membrane decreases as the salt concentration detrimentally buildup at the active-support layer interface due to concentrative internal concentration polarization (ICP).⁴ Hence, the water flux measurements from the latter four stages allow the accurate determination of the resistance to mass transfer in the membrane support layer (i.e., the structural parameter).

Initially the system was equilibrated by circulating DI water across the membrane on both the feed and draw side. To initiate the first stage of the characterization experiment, an appropriate

amount of concentrated NaCl stock solution was dosed into the draw solution to achieve the required salt concentration. Water flux and draw solute reverse flux were recorded at 1 min intervals for 10 min after the fluxes had stabilized (~20 min). Water flux, J_w , was determined by monitoring the rate of change in the draw solution weight, and salt flux, J_s , was calculated from the change in feed solution concentration and the volume of feed water permeated across to the draw side.¹ More concentrated NaCl stock solution was then added to the draw side in the second stage to further raise the concentration and, again, the stabilized second stage J_w and J_s were recorded. The process of increasing the draw solution concentration and taking the steady flux measurements was repeated for the third and fourth stages.

At the start of the fifth stage, a suitable dose of concentration NaCl stock solution is added to the feed solution to decrease the salt concentration difference across the membrane. The osmotic driving force across the membrane diminishes correspondingly, and the reduced water flux is recorded for 10 min after it had stabilized (~15 min). Note that J_s is not recorded here as the relative higher feed solution salt concentration renders the conductivity measurements insensitive to the relatively small increases due to reverse draw solute flux. The steps of adding salt to the feed side and measuring J_w were repeated for the sixth, seventh, and eighth stages. Over the eight stages, the characterization experiment yields a total of twelve flux measurements (eight J_w and four J_s).

The governing equations for J_w and J_s in PRO were derived in our earlier work:⁴

$$J_w = A \left\{ \frac{\pi_D \exp\left(-\frac{J_w}{k}\right) - \pi_F \exp\left(\frac{J_w S}{D}\right)}{1 + \frac{B}{J_w} \left[\exp\left(\frac{J_w S}{D}\right) - \exp\left(-\frac{J_w}{k}\right) \right]} - \Delta P \right\} \quad (1)$$

$$J_s = B \left\{ \frac{c_D \exp\left(-\frac{J_w}{k}\right) - c_F \exp\left(\frac{J_w S}{D}\right)}{1 + \frac{B}{J_w} \left[\exp\left(\frac{J_w S}{D}\right) - \exp\left(-\frac{J_w}{k}\right) \right]} \right\} \quad (2)$$

where c_D and c_F are the draw and feed solution salt concentrations, respectively, π_D and π_F are the respective osmotic pressures, k is the draw solute mass transfer coefficient, D is the NaCl

bulk diffusion coefficient, and ΔP is the hydraulic pressure applied on the draw solution. The water permeability coefficient, A , and salt permeability coefficient, B , are intrinsic properties of the membrane active layer. The support layer structural parameter, S , is defined as $t_s \tau / \varepsilon$, (with t_s being the thickness of the support layer, τ its tortuosity, and ε its porosity) and is characteristic distance a solute molecule must travel through the support layer when going from the active-support layer interface to the bulk feed solution.^{2,6,7}

The membrane properties A , B , and S can be determined numerically by solving the system of twelve equations, i.e., eight water fluxes (eq 1) and four salt fluxes (eq 2), through non-linear regression of the fitting parameters A , B , and S to the measured fluxes (least-squares minimization of the residuals method). The applied pressure, ΔP , is zero in the characterization experiments, k is calculated from correlations for the crossflow cell geometry,⁸ D is determined from literature,⁹ and c_D and c_F were measured with calibrated conductivity meters. The osmotic pressures, π_D and π_F , were determined using the van't Hoff equation, $\pi = \nu c R_g T$, where ν is the number of ionic species each solute molecule dissociates into, R_g is the gas constant, and T is the absolute temperature. Further details of the regression method can be found in our recent publication, together with discussions on the expected accuracy and sensitivity of the calculated parameters.¹ Each membrane was characterized three times: before and after the fouling experiment, and after osmotic backwash cleaning.

RESULTS AND DISCUSSION

Fabricated Membrane Transport and Structural Parameters. Representative scanning electron microscope (SEM) cross-sectional images of the TFC-PRO membranes are presented in Figure S2. The hand-cast membranes comprise an ultra-thin selective polyamide layer, approximated to be ~150 nm thick,⁵ formed by interfacial polymerization on top a support layer ($131 \pm 4 \mu\text{m}$, measured by a digital micrometer) made by phase inversion of polysulfone onto a commercial polyester fabric. An inspection of the micrograph shows large fingerlike macrovoids (10-25 μm width) spanning almost the entire support layer thickness. Previous studies demonstrated that this specific structure facilitates the diffusion of salt within the porous

support, hence minimizing the detrimental effects of internal concentration polarization for enhanced performance in osmotic processes.^{2,3}

The characterization protocol presented in our recent publication¹ was adopted and modified to determine the active layer transport properties and support layer structural parameter intrinsic to the membrane. Table 1 of the manuscript shows the water permeability, A , salt permeability, B , and structural parameter, S , of duplicate hand-cast membranes (TFC-PRO #A and #B). The membrane duplicates possessed similar characteristic parameters, within experimental variations of the hand-casting fabrication technique, and are comparable to literature.³ The structural parameter can be regarded as the characteristic distance a solute particle must diffuse from the active layer-porous support interface of the membrane to reach the bulk feed solution. By thoughtful control of the support layer fabrication conditions, the hand-cast membranes achieved relatively low S values ($505 \pm 37 \mu\text{m}$). This enables the fabricated membranes to minimize ICP detrimental effects, thereby allowing for higher water flux and greater power density performance in PRO.^{4,5}

The J_w and J_s predicted by the calculated membrane parameters in Table 1 are in excellent agreement with experimental measurements for both membrane duplicates, and in all characterizations (i.e., pristine, fouled, and cleaned). Figure S3 of the Supporting Information, top row, shows the experimental fluxes measured in the characterization experiments. The corresponding coefficients of determination, R^2 , indicators of the goodness of fit, fall between 0.965 and 0.999 (average of 0.988 for three tests each on the two hand-cast membranes) and are presented beside each set of fluxes. Figure S3, bottom row, also shows the ratios of J_w to J_s (i.e., reverse flux selectivity) in the first four stages of the characterization protocol. The coefficient of variation (CV) of J_w/J_s is a gauge of the experimental data quality. A low CV signifies that the recorded J_w and J_s measurements are consistent with the governing transport equations in PRO and, hence, the non-linear regression would yield more accurate membrane parameters A , B , and S .¹ For the three characterizations on TFC-PRO #A and #B, the average CV is a low 2.8%.

References

- (1) Tiraferri, A.; Yip, N. Y.; Straub, A. P.; Romero-Vargas Castrillon, S. Elimelech, M., A method for the simultaneous determination of transport and structural parameters of forward osmosis membranes. *Journal of Membrane Science* **2013**, *444*, 523-538.
- (2) Yip, N. Y.; Tiraferri, A.; Phillip, W. A.; Schiffman, J. D. Elimelech, M., High Performance Thin-Film Composite Forward Osmosis Membrane. *Environmental Science & Technology* **2010**, *44* (10), 3812-3818.
- (3) Tiraferri, A.; Yip, N. Y.; Phillip, W. A.; Schiffman, J. D. Elimelech, M., Relating performance of thin-film composite forward osmosis membranes to support layer formation and structure. *Journal of Membrane Science* **2011**, *367* (1-2), 340-352.
- (4) Yip, N. Y.; Tiraferri, A.; Phillip, W. A.; Schiffman, J. D.; Hoover, L. A.; Kim, Y. C. Elimelech, M., Thin-Film Composite Pressure Retarded Osmosis Membranes for Sustainable Power Generation from Salinity Gradients. *Environmental Science & Technology* **2011**, *45* (10), 4360-4369.
- (5) Yip, N. Y. Elimelech, M., Performance Limiting Effects in Power Generation from Salinity Gradients by Pressure Retarded Osmosis. *Environmental Science & Technology* **2011**, *45* (23), 10273-10282.
- (6) McCutcheon, J. R. Elimelech, M., Modeling water flux in forward osmosis: Implications for improved membrane design. *Aiche Journal* **2007**, *53* (7), 1736-1744.
- (7) Phillip, W. A.; Yong, J. S. Elimelech, M., Reverse Draw Solute Permeation in Forward Osmosis: Modeling and Experiments. *Environmental Science & Technology* **2010**, *44* (13), 5170-5176.
- (8) Hoek, E. M. V.; Kim, A. S. Elimelech, M., Influence of crossflow membrane filter geometry and shear rate on colloidal fouling in reverse osmosis and nanofiltration separations. *Environmental Engineering Science* **2002**, *19* (6), 357-372.
- (9) Lobo, V. M. M., Mutual Diffusion-Coefficients in Aqueous-Electrolyte Solutions (Technical Report). *Pure and Applied Chemistry* **1993**, *65* (12), 2614-2640.

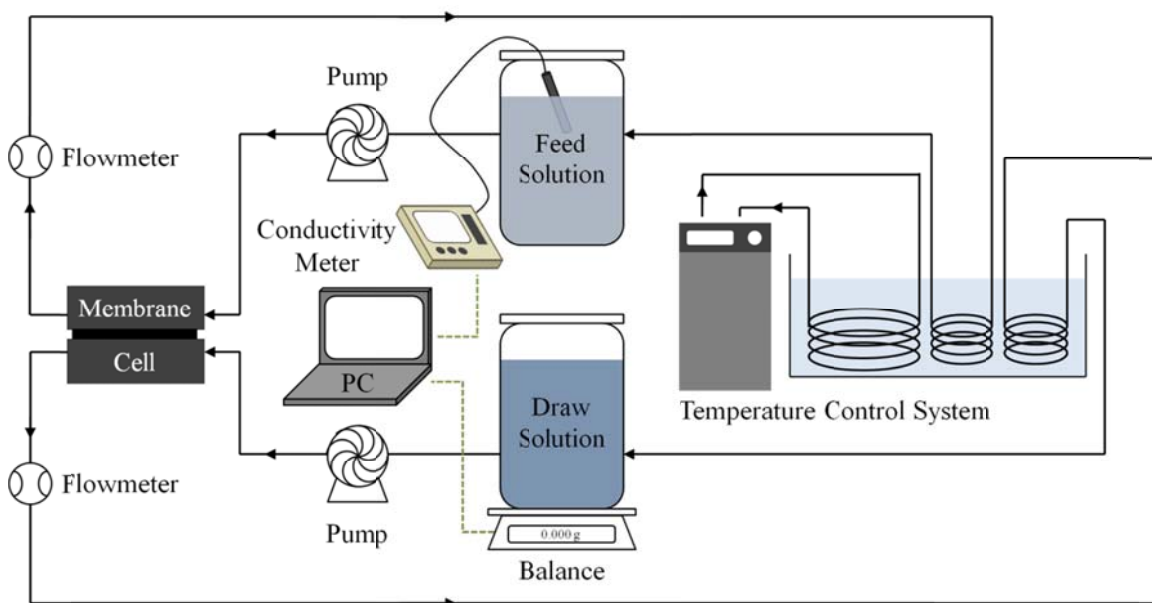


Figure S1. Schematic diagram of the laboratory-scale PRO system. The draw and feed solutions are circulated across the active and support layer of the hand-cast TFC membrane, respectively, in the membrane cell. The water flux is calculated using the gain in weight of the draw solution measured with an analytical scale. The reverse draw salt flux is determined by recording the rate of increase of the feed solution conductivity. The temperature of the system is maintained at $25 \pm 0.5^\circ\text{C}$ for all characterization experiments, and at $25 \pm 1.5^\circ\text{C}$ for other experimental runs.

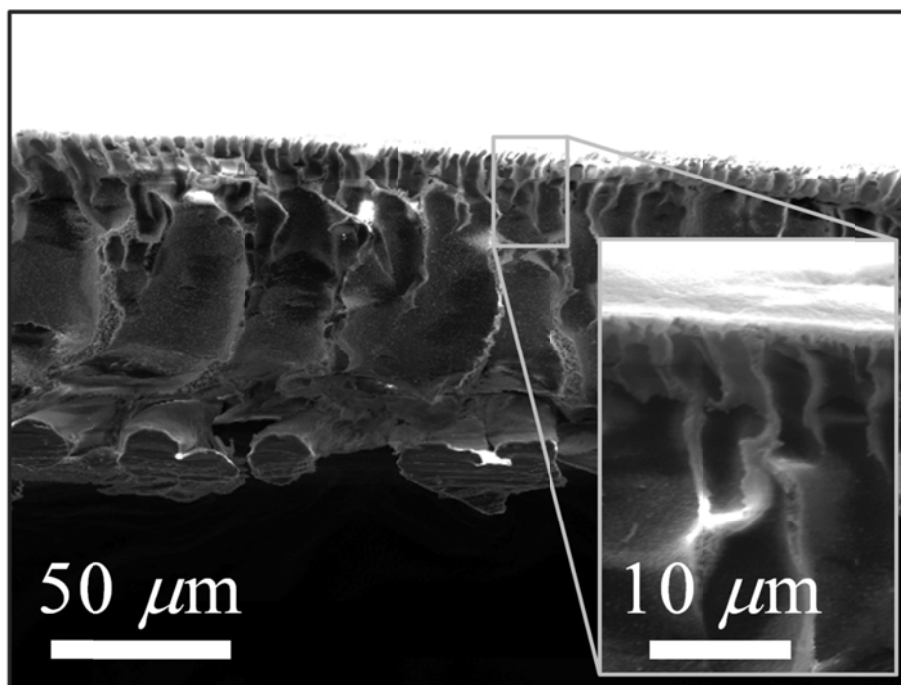


Figure S2. SEM cross-sectional micrograph of a fabricated TFC-PRO membrane. The support layer is relatively thin and possesses a highly porous morphology with finger-like macrovoids that extend across the support layer thickness. The inset shows the magnified view of the skin layer at the top of the porous support with dense, spongelike morphology (magnified view is representative and does not correspond to the actual location on the main micrograph).

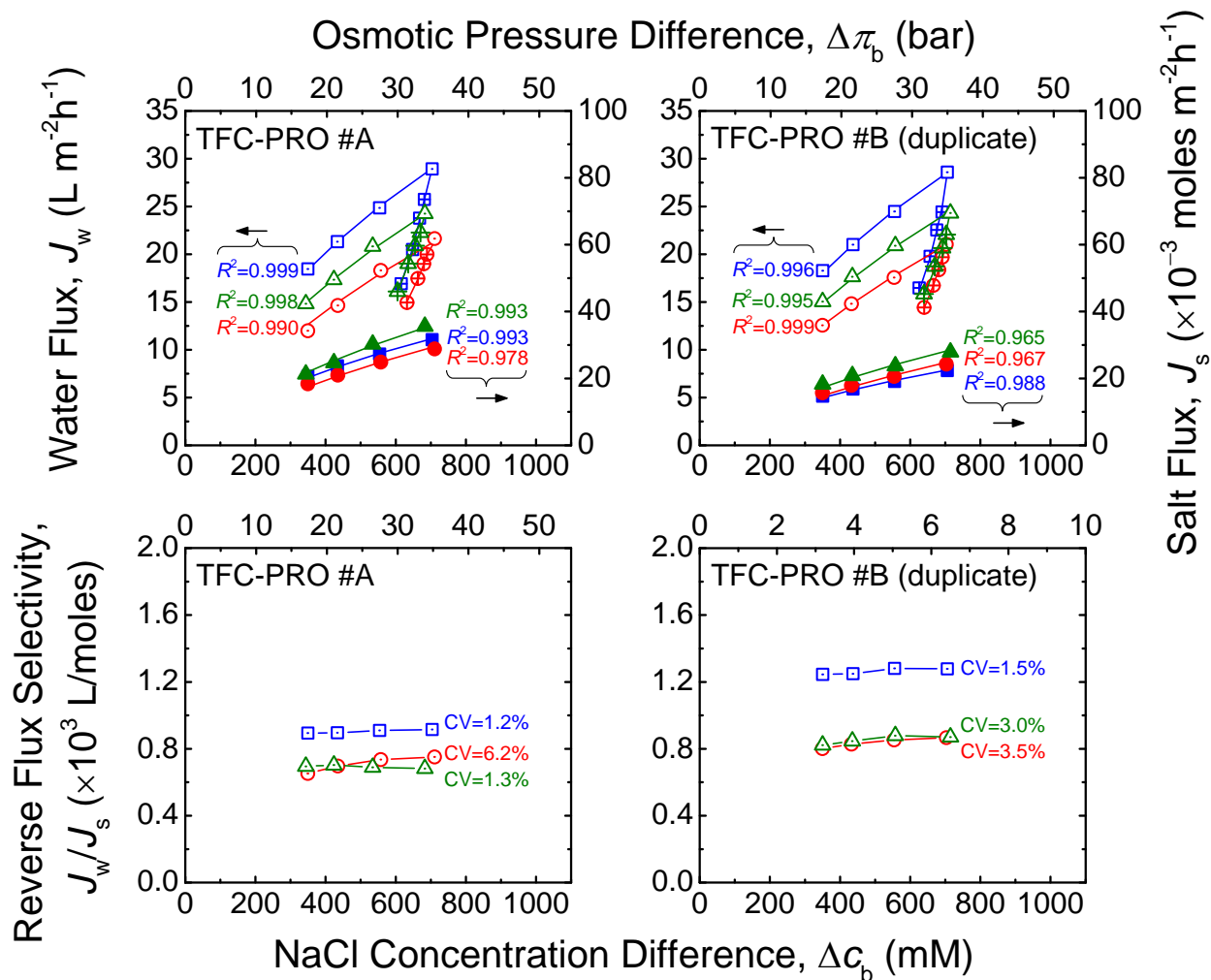


Figure S3. Top row: water flux, J_w , and reverse draw salt flux, J_s , (left and right vertical axes, respectively) as a function of the bulk NaCl salt concentration difference, Δc_b , and corresponding osmotic pressure difference, $\Delta \pi_b$, across the membrane (top and bottom horizontal axes, respectively), in the eight stages of the membrane characterization protocol for hand-cast TFC membranes #A and #B (left and right, respectively). The values beside each series of data points denote the coefficient of determination (R^2) of the predicted water and salt fluxes calculated using the determined membrane parameters compared to the measured experimental fluxes. Bottom row: the ratio of the water flux to the reverse draw salt flux (i.e., reverse flux selectivity) as a function of Δc_b and $\Delta \pi_b$ (top and bottom horizontal axes, respectively) for the first four stages of the characterization protocol. The values beside each set of data points indicate

coefficient of variation (CV) of J_w/J_s . For both the top and bottom rows, the blue square, red circle, and green triangle symbols indicate the values for pristine, fouled, and cleaned membrane, respectively. Empty and crossed symbols represent flux data in the first and last four stages of the characterization protocol, respectively. The mass transfer coefficient of the external concentration polarization boundary layer is calculated using empirical equation to be $13.4 \mu\text{m/s}$, and osmotic pressure is determined with the salt concentration using the van't Hoff relationship.

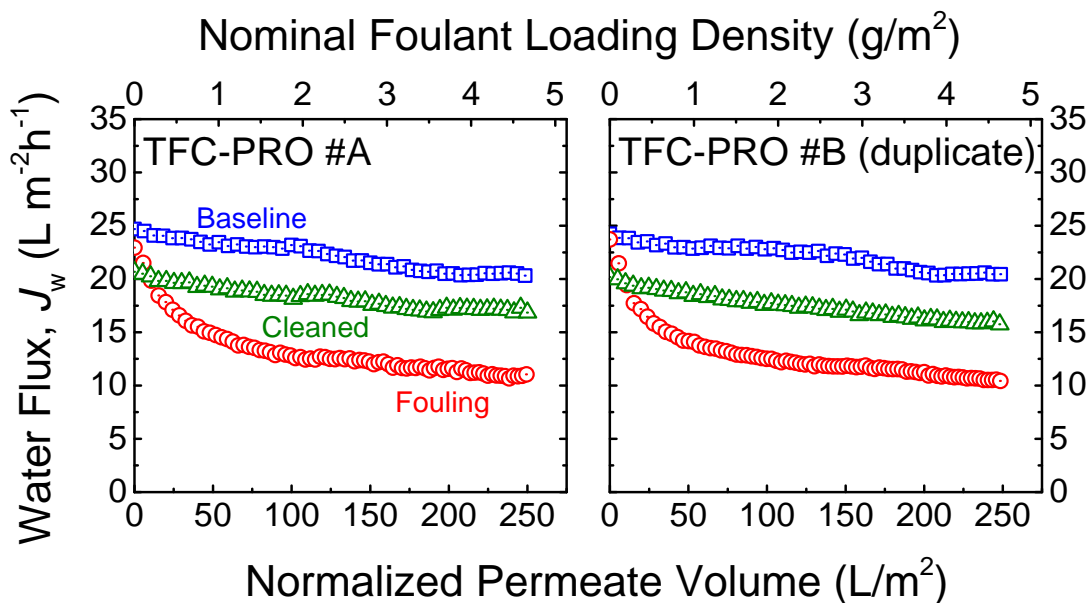


Figure S4. Water fluxes of hand-cast TFC-PRO membranes #A and #B as a function of the permeate volume, normalized by the membrane area, in the baseline, fouling, and cleaned membrane experiments (blue square, red circle, and green triangle symbols, respectively). The model river water composition is 0.4 mM NaCl, 0.2 mM NaHCO₃, and 0.3 mM CaCl₂ (total ionic strength = 1.5 mM), while the model seawater is an NaCl solution (concentration of 570 mM and 590 mM for membranes #A and #B, respectively, to obtain an initial water flux of 25 L m⁻²h⁻¹ in the baseline run). During the fouling experiment, 20 mg/L (nominal) SRNOM was additionally introduced to the river water as model foulant (feed solution pH = 6.96). Crossflow velocity was set at 10.7 cm/s in both membrane channels (no spacers) and the system temperature was maintained at 25 ± 1.5 °C. Each data point represents the average water flux for 15 min periods. The top horizontal axis indicates the nominal foulant loading density into the membrane porous support (initial foulant concentration multiplied by permeate volume). The water fluxes shown are not corrected for dilution of the draw solution during progress of the PRO fouling experiments, thus giving rise to the steady decline in J_w of the baseline and cleaned experiments.

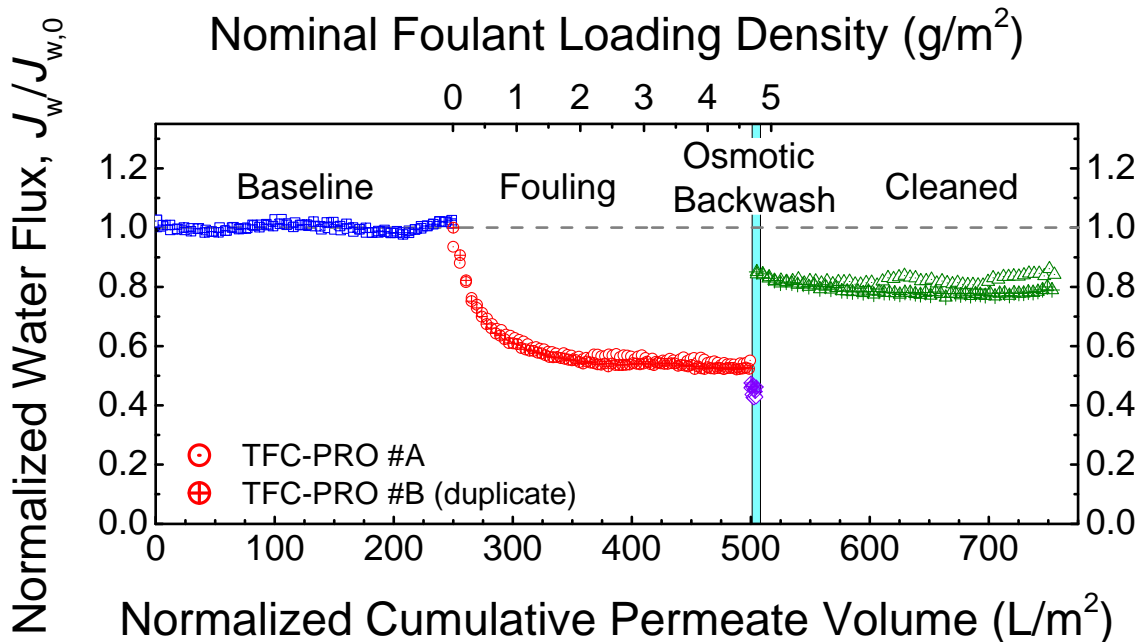


Figure S5. Water flux as a function of the cumulative permeate volume per unit active area of TFC-PRO membranes #A and #B (empty and crossed symbols, respectively). The water flux for the baseline, fouling, osmotic backwash, and cleaned experiments (blue square, red circle, violet diamond, and green triangle symbols, respectively) is normalized to the baseline $J_{w,0}$ to account for the dilution of the draw solution. The experimental conditions are described in Figures 1A and S4. Osmotic backwash was performed by switching the feed and draw streams for 5 L/m^2 of normalized cumulative permeate volume. The top horizontal axis indicates the nominal foulant loading density into the membrane porous support (initial foulant concentration multiplied by permeate volume per unit membrane area) during fouling. Each data point of the baseline, fouling, and cleaned experiment represents the average water flux for 15 min periods, while each data point of the osmotic backwash indicates the average water flux for 5 min intervals. The water fluxes behavior of hand-cast membranes #A and #B are very similar, as evident in the almost complete overlap of the data points in the baseline, fouling, osmotic backwash, and cleaned experimental runs. At the end of the fouling run, normalized water flux declined to 54.4% and 52.5% for #A and #B, respectively, relative to the baseline due to organic fouling of the membrane support layer. Approximately 61.3% and 55.3% of the water flux performance lost to fouling is recovered after the quick osmotic backwash (average water flux of 10.6 $L m^{-2}h^{-1}$ and 10.9 $L m^{-2}h^{-1}$ over ~30 min), for membranes #A and #B, respectively.